Photoacoustics 26 (2022) 100363

Contents lists available at ScienceDirect

Photoacoustics

journal homepage: www.elsevier.com/locate/pacs

Quartz-enhanced photoacoustic NH_3 sensor exploiting a large-prong-spacing quartz tuning fork and an optical fiber amplifier for biomedical applications

Zhijin Shang [a,b,1], Shangzhi Li [a,b,1], Biao Li [a,b], Hongpeng Wu [a,b], Angelo Sampaolo [c], Pietro Patimisco [c], Vincenzo Spagnolo [a,c], Lei Dong [a,b,*]

[a] State Key Laboratory of Quantum Optics and Quantum Optics Devices, Institute of Laser Spectroscopy, Shanxi University, Taiyuan 030006, PR China
[b] Collaborative Innovation Center of Extreme Optics, Shanxi University, Taiyuan 030006, PR China
[c] PolySense Lab-Dipartimento Interateneo di Fisica, University and Politecnico of Bari, Via Amendola 173, Bari, Italy

ARTICLE INFO

Keywords:
Photoacoustic spectroscopy
Quartz tuning fork
Exhaled ammonia monitoring
Breath sensing

ABSTRACT

A sensor system for exhaled ammonia (NH_3) monitoring exploiting quartz-enhanced photoacoustic spectroscopy (QEPAS) was demonstrated. An erbium-doped fiber amplifier (EDFA) with an operating frequency band targeting an NH_3 absorption line falling at 1531.68 nm and capable to emit up to 3 W of optical power was employed. A custom T-shaped grooved QTF with prong spacing of 1 mm was designed and realized to allow a proper focusing of the high-power optical beam exiting the EDFA between the prongs. The performance of the realized sensor system was optimized in terms of spectrophone parameters, laser power and modulation current, resulting in a NH_3 minimum detectable concentration of 14 ppb at 1 s averaging time, corresponding to a normalized noise equivalent absorption coefficient (NNEA) of 8.15×10^{-9} cm^{-1} $W/\sqrt{Hz}$. Continuous measurements of the NH_3 level exhaled by 3 healthy volunteers was carried out to demonstrate the potentiality of the developed sensor for breath analysis applications.

1. Introduction

In the field of medical diagnostics, an increasing number of studies have demonstrated that pathological diagnosis based on respiratory analysis is non-invasive and reliable [1–3]. Abnormal elevated levels of metabolites in exhaled breath herald the deterioration of physical conditions. For instance, normally the amount of ammonia (NH_3) exhaled from the alveoli is several hundred parts per billion in concentration, while a rising ammonia level (>1 ppm) exhaled from humans have been linked to kidney and liver failure [4,5]. Narasimhan et al. have confirmed that there is a strong correlation between the level of respiratory ammonia and blood urea nitrogen (BUN) in patients with end-stage renal disease during hemodialysis [6]. Therefore, real-time measurement of ammonia in exhaled breath is not only used as an indicator of renal failure, but also determines the progress of hemodialysis process.

In order to realize continuous and online ammonia monitoring in exhaled breath, there are two main sensor requirements: (1) ppb-level detection sensitivity; (2) fast response time. Up to now, various technologies for detection of ammonia have been reported, such as carbon nanomaterials [7], chemiluminescence analysis [8], photocatalytic technology [9] and ion chromatography method [10]. However, the presence of interfering substance (molecular impurities, electrolytes and nitrogen oxide) can adversely affect the accuracy of these methods. Moreover, most of these methods have long response time and poor detection sensitivity. Laser-based spectroscopic methods have been widely demonstrated to provide high detection sensitivity and fast measurement time [11–14]. Cavity ring-down spectroscopy (CRDS) is a direct absorption spectroscopy technique, in which laser is injected into a high-precision optical cavity composed of ultra-high reflectivity mirror. The intensity of laser exiting the cavity decreases exponentially with time, and the corresponding cavity ring-down time depends on the target gas concentrations in the cavity. Compared with traditional absorption spectroscopy techniques, CRDS exhibits high sensitivity

* Corresponding author at: State Key Laboratory of Quantum Optics and Quantum Optics Devices, Institute of Laser Spectroscopy, Shanxi University, Taiyuan 030006, PR China.
E-mail address: donglei@sxu.edu.cn (L. Dong).
[1] These authors contributed equally to this manuscript.

https://doi.org/10.1016/j.pacs.2022.100363
Received 5 February 2022; Received in revised form 24 April 2022; Accepted 28 April 2022
Available online 4 May 2022

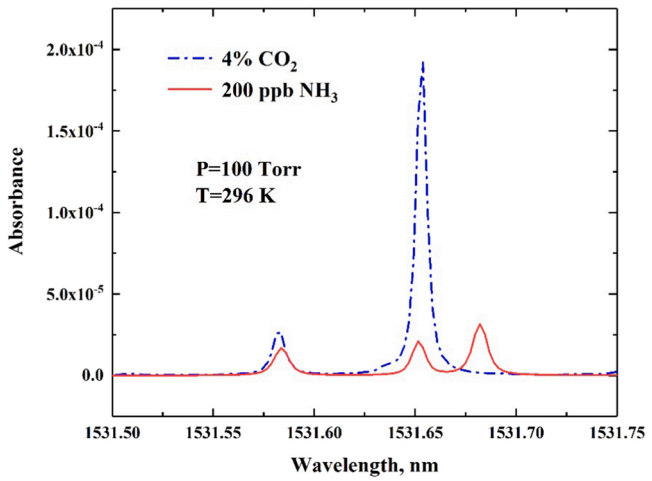

Fig. 1. Simulated absorbance of 200 ppb NH_3 (solid line) and 4% CO_2 (dash-dotted line) at a pressure of 100 Torr.

because it is not affected by variations in the incident laser intensity and benefits from long effective optical paths. For example, Manne et al. have implemented a similar technique to achieve a sensitivity of 50 parts per billion for ammonia detection [4]. However, the large volume of the optical cavity causes a long retention time for target gas, resulting in a degraded time resolution of 20 s, which is inappropriate for applications requiring continuous and real-time gas monitoring of exhaled breath.

Photoacoustic spectroscopy (PAS) is another well-established technique owing to its relatively simple, real-time and zero-background signal [15–17], in which the optoacoustic signal is detected by broadband microphones to retrieve the trace gas concentration levels. Quartz-enhanced photoacoustic spectroscopy (QEPAS), an improved version of traditional PAS, employs a small-size, high-Q-factor quartz tuning fork (QTF) instead of a conventional microphone as a resonant acoustic transducer. The key innovation of QEPAS is the use of the QTF with high resonance frequency (up to several kHz) and narrow frequency band (few Hz or less), which results in an improved immunity of the QEPAS system to ambient noise [18–49]. Moreover, QEPAS has a simple spectrophone design and is capable to analyze trace-gas samples of few mm^3 in volume, providing a high detection sensitivity level and fast response time, and hence is very suitable for detecting exhaled gas in real time, as demonstrated in [35,36].

A remarkable feature of QEPAS is that its detection sensitivity is in direct proportion to the optical excitation power, which provides an approach to further improve QEPAS detection sensitivity by employing high-power lasers or optical fiber amplifiers [37,38]. Nowadays commercially available erbium-doped fiber amplifiers (EDFAs) with sophisticated technology have three telecommunication bands, i.e., S band (1450–1550 nm), C band (1520–1570 nm) and L band (1565–1610 nm). The first combination of a QTF-based QEPAS sensor and an EDFA for H_2S detection has been reported [39]. However, due to the limitation of 300-μm prong spacing of QTF and the degraded beam quality caused by the EDFA, a large background noise was introduced.

In this manuscript, a NH_3 sensor system aiming at real-time respiration monitoring is demonstrated, in which a novel custom QTF with prong spacing of 1 mm and an EDFA in the wavelength range of 1531–1540 nm were employed. Benefiting from the high output power of the EDFA, the wide prong spacing of the custom QTF and the small size of the QEPAS cell, a ppb-level detection sensitivity and rapid response time were achieved. To demonstrate its effectiveness for breath analysis applications, the NH_3 QEPAS sensor was tested by measuring the ammonia levels exhaled by three healthy individuals.

2. Selection of target absorption line

Due to the presence of the fingerprint spectrum of gas molecules, the QEPAS technology based on Beer Lambert's law enables excellent selectivity as well as real-time measurement. Ammonia has a complex infrared spectrum with four fundamental vibrational modes (ν_1, ν_2, ν_3, ν_4). According to the HITRAN database, NH_3 two perpendicular bands ($\nu_1+\nu_3$, $2\nu_3^2$) are dominant in the vicinity of 1.5 μm [40]. There are three strong absorption lines in the wavelength range 1531.5–1531.75 nm, whose simulated absorbances are plotted in Fig. 1. Two of three lines overlap with two weak neighboring absorption lines of carbon dioxide (CO_2). Since the content of CO_2 exhaled from the alveoli of a healthy individual is ~4%, far higher than the exhaled level of ammonia, concentration levels of 4% and 200 ppb, at a pressure of 100 Torr, were used for CO_2 (dash-dotted line) and NH_3 (solid line), respectively, in the generated spectra shown in Fig. 1. Operating at low pressure is helpful in reducing the pressure broadening effect and avoiding spectral overlaps between the absorption lines. The interference-free ammonia line at 1531.68 nm ($\bar{\nu}$= 6528.77 cm^{-1}) with an absorption line strength of 1.174×10^{-21} cm/molecule was selected as target line.

3. Design of custom QTF for EDFA

To realize the photoacoustic sensor system, an EDFA was employed, offering an adjustable output power from 20 mW to 3 W without variation of the laser wavelength. Being the QEPAS signal proportional to the selected absorption line strength, in terms of detection sensitivity, the watt-level amplified output power of the EDFA can effectively compensate the NH_3 low absorption line strengths falling in the near-IR spectral region, which are about two orders of magnitude weaker than the corresponding lines falling in the mid-IR range. Moreover, the commercial availability of mid-IR semiconductor laser sources, such as

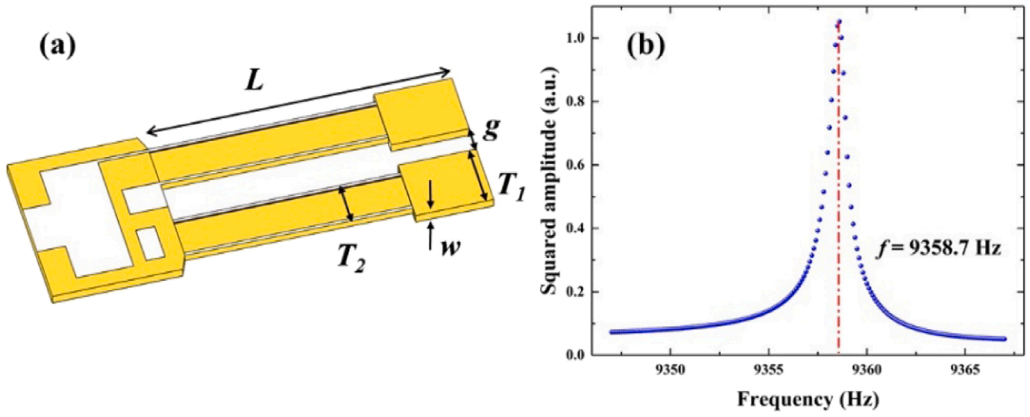

Fig. 2. (a) Schematic diagram of the T-shaped QTF. (b) Frequency response curve of the T-shaped grooved QTF at atmospheric pressure.

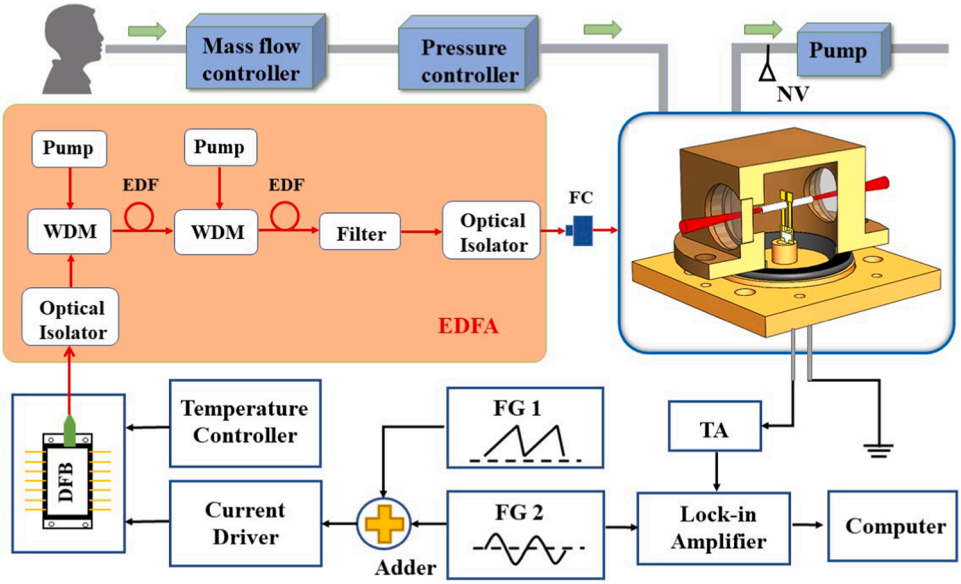

Fig. 3. Schematic of the QEPAS-based sensor system for exhaled ammonia detection. EDFA: Erbium-doped fiber amplifier; NV: needle valve; FG: Function Generator; TA: Transimpedance Amplifier; WDM: Wavelength Division Multiplexing.

quantum cascade lasers, has a high cost and heat dissipation issue, the combination of a small sized and low-cost near-infrared DFB lasers with an EDFA is an alternative technology. The design of the custom QTF for the EDFA needs to consider three aspects: (1) large prong spacing to match the high-power laser beam exiting the EDFA; (2) a high Q factor to achieve a high sensitivity; (3) a low resistance to enhance the piezoelectric conversion efficiency of the QTF.

Based on the laser beam quality of the EDFA, a prong spacing of 1 mm is large enough to effectively reduce the background noise generated by tail of the optical beam hitting the QTF [18]. A hammer-like structure was designed on the QTF tine, increasing the top weight of the QTF and thus increase the generated prongs stress field. An increase of the amplitude of the stress field produces an increase of the piezoelectrically induced charges, and subsequently an enhancement of the QTF current signal. The reported QTF is referred as T-shaped grooved QTF, whose schematic and geometrical parameters are shown in Fig. 2(a). The prong length *L*, thickness *w*, and prong spacing *g* of the T-shaped grooved QTF are 9.4 mm, 2 mm, and 1 mm, respectively. The width of the hammer-shaped part T_1 and non-hammer-shaped part T_2 of the QTF prongs are 2 mm and 1.4 mm, respectively. In addition, four 50-μm deep rectangular grooves was carved on the surface of each QTF prong, decreasing the distance between two electrodes and leading to a low QTF resistance, thereby increasing the generated signal [18]. The response curve of the T-shaped grooved QTF is shown in Fig. 2(b). At a pressure of 100 Torr, the resonant frequency, quality factor, and equivalent resistance of the QTF are 9358.7 Hz, 15,866, and 139.2 kΩ, respectively.

4. Photoacoustic sensor system

The schematic diagram of the EDFA-based QEPAS sensor for exhaled ammonia detection is depicted in Fig. 3. A near-infrared distributed feedback (DFB) diode laser (NTT Electronics Corporation model NLK1C5J1AA) with a center emission wavelength of 1531.68 nm served

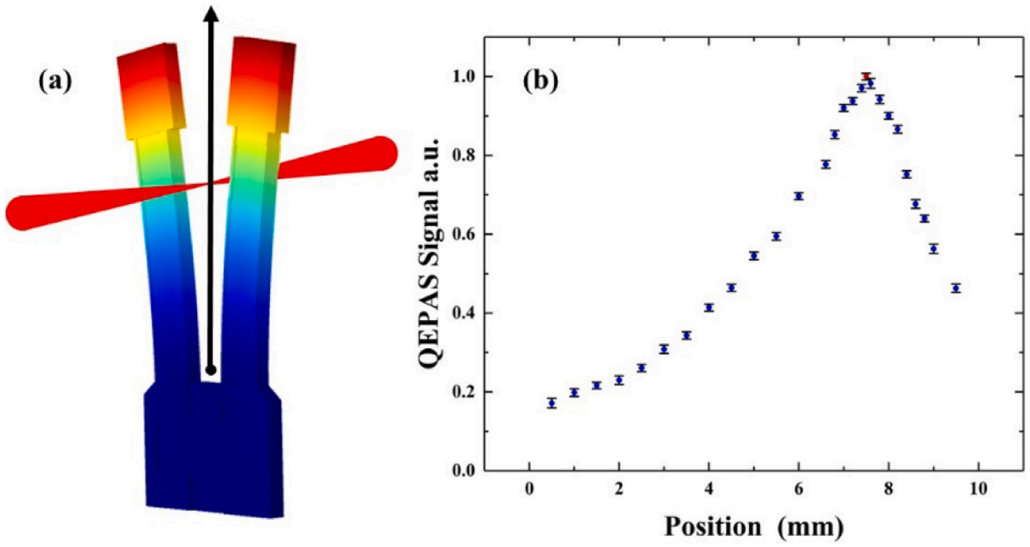

Fig. 4. (a) Sketch of a QTF depicting the prong deformation when the laser is focused on the QTF symmetry axis (Black arrow). (b) Normalized QEPAS signals obtained at different laser focal point locations. The positions on the x-axis are measured starting from the prongs bottom.

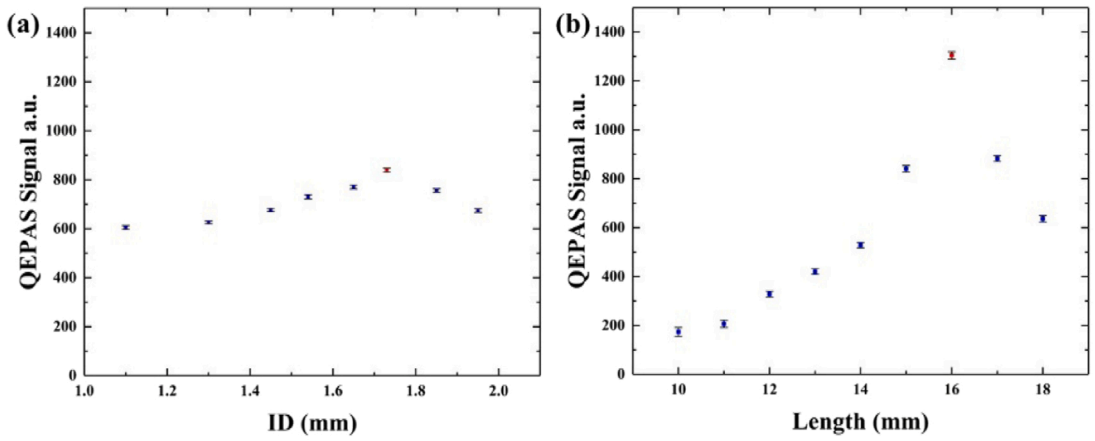

Fig. 5. (a) The relationship between the normalized QEPAS signal and the ID of the AmRs, ID: inner diameter of the tube. (b) The normalized QEPAS signal as a function of tube length.

as the excitation source. The temperature controller and current driver are integrated on the drive board to control the output wavelength of the laser. The 30 mHz ramp signal generated from a function generator slowly scans the laser wavelength across the absorption line of interest. In addition, the current of the laser was sinusoidally modulated at $f_0/2$, where f_0 was the resonance frequency of the custom QTF. The laser beam with an output power of 20 mW was directed to the C-band EDFA (BKtel THPOA-SP400ac-FCAPC) with a two-stage amplifier, which has an output power stability of $< 2\%$. Two optical isolators were utilized at the entrance and exit of the EDFA to protect the DFB diode laser against back reflections. The outgoing laser beam was collimated by a fiber-coupled collimator (FC) with a transmittance of 95% at ~1.5 μm, resulting in a collimating laser beam with a diameter of 650 μm, which allowed the laser beam to easily pass through the QTF prongs without hitting their surfaces.

The excited photoacoustic signal was detected by the custom QTF and amplified by a low noise trans-impedance amplifier with a 10-MΩ feedback resistor. Then the amplified signal was demodulated by the lock-in amplifier (Stanford Research Systems, model SR830) in the 2*f* mode with regards to the synchronous reference signal provided by the function generator (FG2). The time constant and slope filter of this lock-in amplifier were 300 ms and 12 dB/oct, respectively, resulting in a detection bandwidth of 0.833 Hz. The gas pressure in the 70 cm^3 gas cell was controlled at 100 Torr by a compact pressure controller (MKS Instrument Inc., U.S.A., Model 649B) in all measurements. The flow of human exhaled gas was set to a constant value of 80 sccm, which is the available maximum flow rate due to the low pressure. A flowmeter (Alicat Scientific, Inc. Model M-500SCCMD) was used to monitor the gas flow rate simultaneously.

As shown in Fig. 4(a), the optimal sound excitation position for the QTF were determined by comparing the QEPAS signals generated by the laser beam focusing at different positions along the QTF symmetry axis. The experimental QEPAS signals, normalized to the maximum value and measured as a function of the laser focus positions, are shown in Fig. 4 (b). The optimal laser focus position was determined to be 7.5 mm away from the bottom of the QTF prongs.

Significant enhancements of the QEPAS signal-to-noise ratio have can been obtained by implementing acoustic micro-resonators (AmRs) in on-beam QEPAS. For this configuration an AmR typically consists of two stainless steel tubes with the QTF positioned perpendicularly between them to probe the acoustic vibration excited in the gas contained inside the tubes [18]. The distance between the QTF and the tubes was set at 100 μm and the geometric parameters of the AmR were optimized. The normalized QEPAS signal vs the AmRs inner diameter (ID) is shown in Fig. 5(a). The optimum ID of the AmRs was determined to be 1.7 mm. Since the cross-sectional dimensions of the optimum AmR are much smaller than the acoustic wavelength ($\lambda_s \cong 37.8$ mm for $f_0 \cong$ 9 kHz), a standing wave propagating longitudinally along the resonator was just excited, generating a one-dimensional acoustic field.

By optimizing the length of the single tube, the first-order longitudinal mode of the acoustic wave can match the resonance frequency of the QTF. According to the theory published in Ref [25], the optimum length of each tube is between $\lambda_s/2$ and $\lambda_s/4$, where λ_s is the sound wavelength. As shown in Fig. 5(b), the normalized QEPAS signal rises at

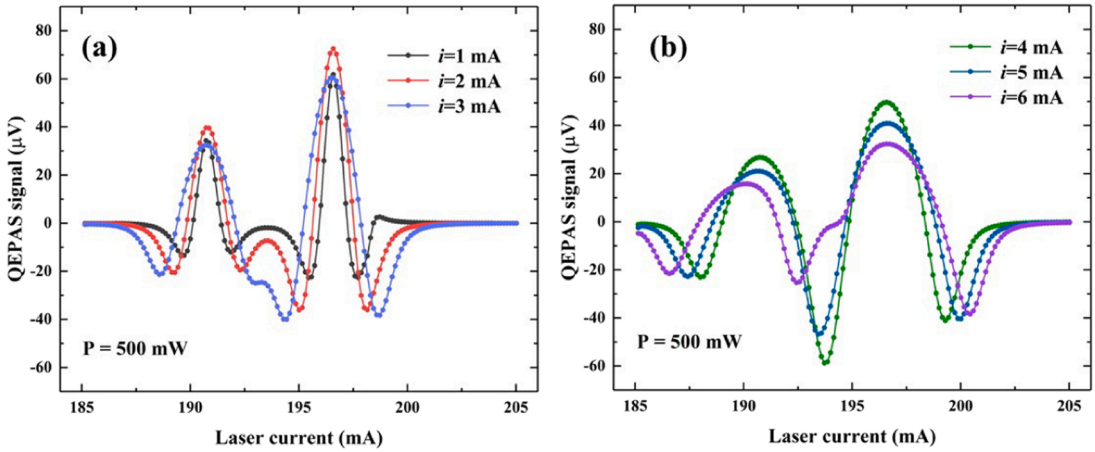

Fig. 6. The 2*f* signal measured at different modulation currents from 1 mA to 3 mA (a) and 4–6 mA (b).

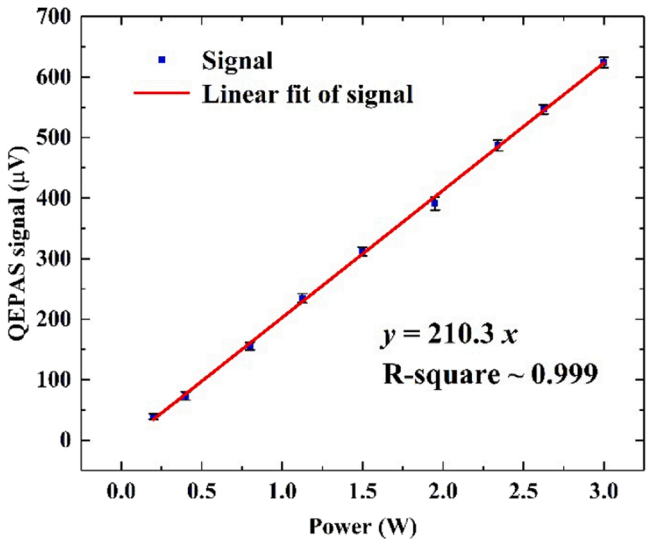

Fig. 7. QEPAS signals peak value as a function of actual excitation power.

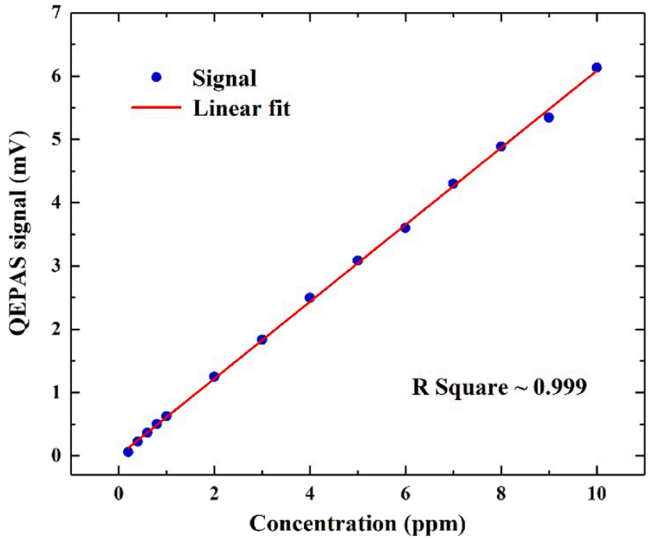

Fig. 8. Amplitudes of the 2*f* signal as a function of the NH_3 concentrations from 0.2 ppm to 10 ppm in air.

increasing the tube length, and then reaches the maximum value at l = 16 mm, where the strongest acoustic coupling between the QTF and the AmRs is obtained.

5. Optimization of experimental parameters

For the QEPAS-based sensor, the signal amplitude is dependent on the laser current modulation depth. Thus, the modulation depth was optimized experimentally to obtain the highest QEPAS signal. A 1 ppm NH_3/air mixture was fed into the chamber as a gas sample and the QEPAS signal was measured at different modulation depths from 1 mA to 6 mA when the laser wavelength slowly sweeps across the target NH_3 absorption line ($\bar{\nu}$= 6528.77 cm^{-1} for I = 196 mA), for an optical emitted power of 500 mW. As shown in Fig. 6, the maximum QEPAS signal was achieved at the modulation current of 2 mA. At larger modulation current the QEPAS signals of the two NH_3 absorption lines at 6528.77 cm^{-1} and 6528.91 cm^{-1} begin to merge. Therefore, an optimal modulation depth of 2 mA was adopted in the following investigations.

The detection sensitivity of the QEPAS-based sensor is proportional to the excitation laser power. However, with laser power increasing, saturation effects may occur, which means that the depletion from the vibrational excited level slows with respect to the pump rate, and thus molecules are unable to be excited to higher energy levels. Thereby, we measured the QEPAS signal vs optical power in the range 200 mW–3 W for 1 ppm NH_3/air mixture, to verify our sensor system was not operated in saturation. The obtained results are shown in Fig. 7.

The signal amplitude increases linearly with the increase of actual excitation power, while the sensor noise was constantly kept at μV level thanks to the large prongs gap of the custom QTF, proving that the sensor is not operated in saturation condition.

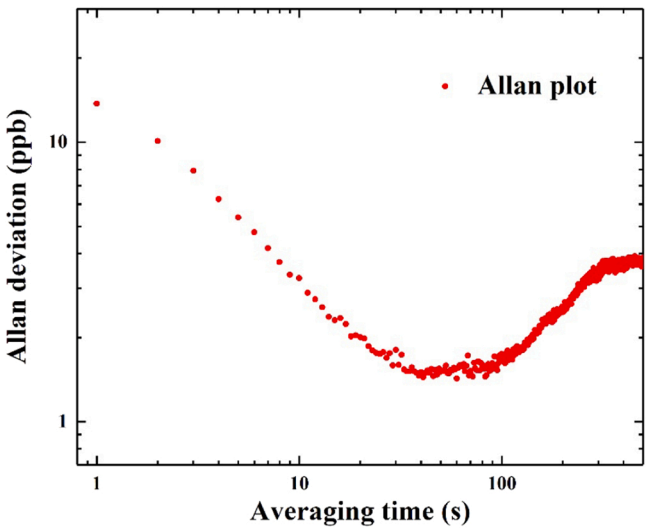

Fig. 9. Allan-Werle deviations as a function of the averaging time for pure air gas samples.

6. Results and discussion

To evaluate the performance of the sensor system for NH_3 detection, the system was operated at the optimized values of modulation depth and the excitation power of 3 W. The peak values of the 2*f* signal have been measured at different NH_3 concentrations, starting from a certified concentration of 10 ppm NH_3:standard air and diluting down to 0.2 ppm in air using a gas mixer with 1.5% of water added and the obtained results are plotted in Fig. 8. Each data point in the figure represents the average of 50 repeated measurements. An *R*-square value of 0.999 was obtained through a linear fit, which confirmed that the sensor system linearly responds to the NH_3 concentration. The sensor noise was defined as the 1 σ standard deviation (2.13 μV) of the signal when the pure air was introduced in the gas cell. With 200-ppb NH_3/air mixture flushed into the system, a minimum detection limit (MDL) of 14 ppb was measured in a detection bandwidth of 0.833 Hz. A normalized noise equivalent absorption (NNEA) value of 8.15×10^{-9} cm^{-1} W/$\sqrt{Hz}$ was achieved.

An Allan-Werle deviations analysis was performed to evaluate the long-term stability of the NH_3 sensor. The gas chamber was filled with air, at a pressure of 100 torr, and the output wavelength of the laser was locked to the NH_3 absorption line at 6528.77 cm^{-1}. The Allan deviation result plotted in Fig. 9 shows that the detection limit of the NH_3 sensor can be improved if increasing the averaging time. For an averaging time up to 40 s, the Allan–Werle deviation plots follows a $1/\sqrt{t}$ dependence, which means that the white noise of the sensor is the dominant noise source. At an averaging time of 40 s an NH_3 MDL of 1.5 ppb has been achieved.

These performances pave the way to the application of the developed sensor system for environmental and biomedical applications. As proof of this last statement, the NH_3 sensor system was successfully tested for online detection of human exhaled ammonia. The exhaled breath from

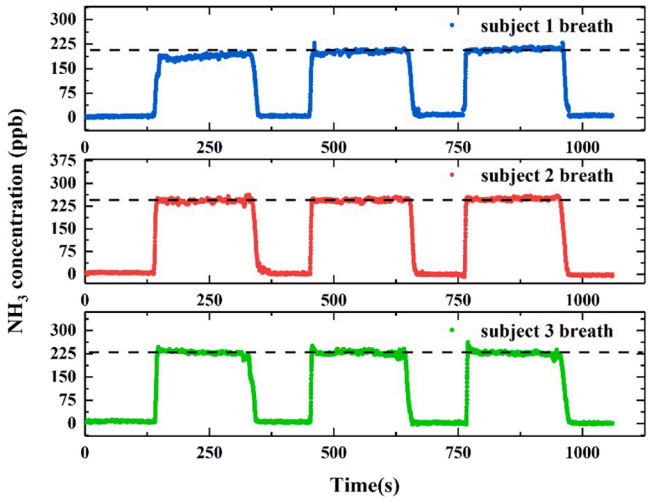

Fig. 10. Online concentration measurements of exhaled ammonia by three healthy subjects.

three volunteers was introduced into the gas chamber in real time by a custom exhaled gas sampling apparatus, a Nafion humidifier was inserted inline to keep the water concentration entering the QEPAS cell at 1.5% to eliminate the influence of environmental water vapor changes on the experimental system. A pump located downstream of the gas path was continuously operated to ensure the flow rate and pressure of the gas in the chamber. Fig. 10 shows the measurement results of the exhaled ammonia by 3 healthy subjects. Two minutes after the timer started, the exhaled ammonia gas was collected by the gas sampling apparatus and transmitted to the detection module. The measurement process lasted three minutes for online monitoring of ammonia levels exhaled by the subjects over a long period of time, rather than the changes in the ammonia concentration of the subjects exhaled in one breath.

When the exhaled breath was no longer fluxed into the detection module, the QEPAS decreases rapidly to the noise level, demonstrating that no-memory effects are present. The measurement process of exhaled ammonia by three healthy subjects was repeated three times to verify the stability of the NH_3 sensing system. A signal rise/fall time of ~15 s was achieved and Exhaled ammonia levels in the range 170–230 ppb was observed. The small bumps at the beginning of each detection window in the measurements of the breath of subject 3 reflects the ammonia concentration in the oral cavity. This higher concentration is mostly related to oral bacterial processes of ingested food and beverages [41]. The signal dither observed was caused by instability in respiratory rate.

7. Conclusions

An NH_3 QEPAS sensor implementing an erbium-doped fiber amplifier and a custom T-shaped grooved QTF with prong spacing of 1 mm was demonstrated. Our previous experimental results show that there is a significant background noise from an 800-μm-prong-spacing QTF when the laser power is amplified to watt-levels. Therefore, a novel QTF with a prongs gap of 1 mm was designed here. The wider prongs gap of the custom QTF significantly reduces the photothermal noise caused by the stray light hitting the prongs of QTF. Due to the increase in excitation power, a lower MDL of 14 ppb at 1 s averaging time, corresponding to a NNEA of 8.15×10^{-9} cm^{-1} $W/\sqrt{Hz}$, has been achieved. The MDL reduces to 1.5 ppb if increasing the averaging time to 40 s. The obtained performances allow the implementation of the NH_3 QEPAS sensor for NH_3 monitoring in exhaled human breath. The experimental results confirm the potentiality of the developed NH_3 sensor to be implemented for renal disease screening and monitoring of treatment progress of patients with end-stage renal pathology, whose exhaled ammonia level is usually > 1 ppm.

Declaration of Competing Interest

The authors declare that they have no known competing financial interests or personal relationships that could have appeared to influence the work reported in this paper.

Acknowledgments

The project is sponsored by National Key Research and Development Program of China (No. 2019YFE0118200); National Natural Science Foundation of China (NSFC) (Nos. 62175137, 62122045, 62075119, 61805132); THORLABS GmbH, within PolySense, a joint-research laboratory; Sanjin Scholar (No. 2017QNSJXZ-04), and Shanxi "1331KSC".

References

[1] K. Alving, E. Weitzberg, H. Kollberg, E. Weitzberg, S.L. Nordvall, J.O. Lundberg, Increased amount of nitric oxide in exhaled air of asthmatics, Eur. Respir. J. 75 (4) (1993) 1368–1370.
[2] P. Paredi, W. Biernacki, G. Invernizzi, S.A. Kharitonov, P.J. Barnes, Exhaled carbon monoxide levels elevated in diabetes and correlated with glucose concentration in blood: a new test for monitoring the disease? Chest 116 (4) (1999) 1007–1011.
[3] R.C. Spiller, J.C. Atherton, The urea breath test for Helicobacter pylori, Gut 35 (6) (1994) 723–725.
[4] J. Manne, O. Sukhorukov, W. Jäger, J. Tulip, Pulsed quantum cascade laser-based cavity ring-down spectroscopy for ammonia detection in breath, Appl. Opt. 45 (36) (2006) 9230–9237.
[5] C. Wang, P. Sahay, Breath analysis using laser spectroscopic techniques: breath biomarkers, spectral fingerprints, and detection limits, Sensors 9 (10) (2009) 8230–8262.
[6] L.R. Narasimhan, W. Goodman, C.K. Patel, Correlation of breath ammonia with blood urea nitrogen and creatinine during hemodialysis, Proc. Natl. Acad. Sci. USA 98 (8) (2001) 4617–4621.
[7] R. Ghosh, A. Midya, S. Santra, S.K. Ray, P.K. Guha, Chemically reduced graphene oxide for ammonia detection at room temperature, Appl. Mater. Interfaces 5 (15) (2013) 7599–7603.
[8] H. Chen, H. Li, J. Lin, Determination of ammonia in water based on chemiluminescence resonance energy transfer between peroxymonocarbonate and branched $NaYF_4$:Yb^{3+}/Er^{3+} nanoparticles, Anal. Chem. 84 (20) (2012) 8871–8879.
[9] Y. Zhao, R. Shi, X. Bian, C. Zhou, Y. Zhao, S. Zhang, F. Wu, G.I.N. Waterhouse, L. Wu, C. Tung, T. Zhang, Ammonia detection methods in photocatalytic and electrocatalytic experiments: how to improve the reliability of NH_3 production rates? Adv. Sci. 6 (8) (2019), 1802109.
[10] M.L. Dawson, V. Perraud, A. Gomez, K.D. Arquero, M.J. Ezell, B.J. Finlayson-Pitts, Measurement of gas-phase ammonia and amines in air by collection onto an ion exchange resin and analysis by ion chromatography, Atmos. Meas. Technol. 7 (37) (2014) 2733–2744.
[11] G.P. Wyers, R.P. Otjes, J. Slanina, A continuous-flow denuder for the measurement of ambient concentration and surface-exchange fluxes of ammonia, Atmos. Environ. 27 (13) (1993) 2085–2090.
[12] M.P. Keuken, A. Wayers-Ijpelaan, J.J. Mols, R.P. Otjes, J. Slanina, The determination of ammonia in ambient air by an automated thermodenuder system, Atmos. Environ. 23 (10) (1967) 2177–2185.
[13] M.E. Webber, D.S. Baer, R.K. Hanson, Ammonia monitoring near 1.5 μm with diode-laser absorption sensors, Appl. Opt. 40 (12) (2001) 2031–2042.
[14] R. Claps, F.V. Englich, D.P. Leleux, D. Richter, F.K. Tittel, R.F. Curl, Ammonia detection by use of near-infrared diode-laser-based overtone spectroscopy, Appl. Opt. 40 (24) (2001) 4387–4394.
[15] A. Elia, P.M. Lugarà, C. Di Franco, V. Spagnolo, Photoacoustic techniques for trace gas sensing based on semiconductor laser sources, Sensors 9 (12) (2009) 9616–9628.
[16] M.E. Webber, M. Pushkarsky, C. Kumar, N. Patel, Fiber-amplifier-enhanced photoacoustic spectroscopy with near-infrared tunable diode lasers, Appl. Opt. 42 (12) (2003) 2119–2126.
[17] X. Yin, L. Dong, H. Wu, H. Zheng, W. Ma, L. Zhang, W. Yin, S. Jia, F.K. Tittel, Sub-ppb nitrogen dioxide detection with a large linear dynamic range by use of a differential photoacoustic cell and a 3.5 W blue multimode diode laser, Sens. Actuators B Chem. 247 (2017) 329–335.
[18] P. Patimisco, A. Sampaolo, L. Dong, F.K. Tittel, V. Spagnolo, Recent advances in quartz enhanced photoacoustic sensing, Appl. Phys. Rev. 5 (2018), 011106.
[19] B. Li, C. Feng, H. Wu, S. Jia, L. Dong, Calibration-free mid-infrared exhaled breath sensor based on BF-QEPAS for real-time ammoni a measurements at ppb level, Sens. Actuators. B Chem. 358 (2022) 131510.
[20] A. Sampaolo, S. Csutak, P. Patimisco, M. Giglio, G. Menduni, V. Passaro, F.K. Tittel, M. Deffenbaugh, V. Spagnolo, Methane, ethane and propane detection using a compact quartz enhanced photoacoustic sensor and a single interband cascade laser, Sens. Actuators B Chem. 282 (2019) 952–960.

[21] M. Winkowski, T. Stacewicz, Low noise, open-source QEPAS system with instrumentation amplifier, Sci. Rep. 9 (1) (2019) 1838.
[22] L. Dong, H. Wu, H. Zheng, Y. Liu, X. Liu, W. Jiang, L. Zhang, W. Ma, W. Ren, W. Yin, S. Jia, F.K. Tittel, Double acoustic microresonator quartz-enhanced photoacoustic spectroscopy, Opt. Lett. 39 (8) (2014) 2479–2482.
[23] H. Zheng, L. Dong, A. Sampaolo, H. Wu, P. Patimisco, X. Yin, W. Ma, L. Zhang, W. Yin, V. Spagnolo, S. Jia, F.K. Tittel, Single-tube on-beam quartz-enhanced photoacoustic spectroscopy, Opt. Lett. 41 (5) (2016) 978–981.
[24] F. Wang, J. Chang, Q. Wang, Y. Liu, Z. Liu, Z. Qin, C. Zhu, Improvement in QEPAS system based on miniaturized collimator and flat mirror, Opt. Commun. 381 (2016) 152–157.
[25] S. Li, H. Wu, R. Cui, A. Sampaolo, P. Patimisco, V. Spagnolo, F.K. Tittel, L. Dong, Piezo-enhanced acoustic detection module for mid-infrared trace gas sensing using a grooved quartz tuning fork, Opt. Express 27 (24) (2019) 35267–35278.
[26] M. Giglio, A. Elefante, P. Patimisco, A. Sampaolo, F. Sgobba, H. Rossmadl, V. Mackowiak, H. Wu, F.K. Tittel, L. Dong, V. Spagnolo, Quartz-enhanced photoacoustic sensor for ethylene detection implementing optimized custom tuning fork-based spectrophone, Opt. Express 27 (4) (2019) 4271–4280.
[27] H. Wu, L. Dong, H. Zheng, Y. Yu, W. Ma, L. Zhang, W. Yin, L. Xiao, S. Jia, F. K. Tittel, Beat frequency quartz-enhanced photoacoustic spectroscopy for fast and calibration-free continuous trace-gas monitoring, Nat. Commun. 8 (2017) 15331.
[28] S. Li, L. Dong, H. Wu, A. Sampaolo, P. Patimisco, V. Spagnolo, F.K. Tittel, Ppb level quartz-enhanced photoacoustic detection of carbon monoxide exploiting a surface grooved tuning fork, Anal. Chem. 91 (9) (2019) 5834–5840.
[29] K. Liu, X. Guo, H. Yi, W. Chen, W. Zhang, X. Gao, Off-beam quartz-enhanced photoacoustic spectroscopy, Opt. Lett. 34 (10) (2009) 1594–1596.
[30] A. Sampaolo, P. Patimisco, M. Giglio, A. Zifarelli, H. Wu, L. Dong, V. Spagnolo, Quartz-enhanced photoacoustic spectroscopy for multi-gas detection: a review, Anal. Chim. Acta 338894 (2021).
[31] W. Ren, W.Z. Jiang, F.K. Tittel, Single-QCL-based absorption sensor for simultaneous trace-gas detection of CH_4 and N_2O, Appl. Phys. B 117 (1) (2014) 245–251.
[32] H. Wu, L. Dong, X. Yin, A. Sampaolo, P. Patimisco, W. Ma, L. Zhang, W. Yin, L. Xiao, V. Spagnolo, S. Jia, Atmospheric CH_4 measurement near a landfill using an ICL-based QEPAS sensor with V-T relaxation self-calibration, Sens. Actuators B Chem. 297 (2019), 126753.
[33] H. Wu, A. Sampaolo, L. Dong, P. Patimisco, X. Liu, H. Zheng, X. Yin, W. Ma, L. Zhang, W. Yin, V. Spagnolo, S. Jia, F.K. Tittel, Quartz enhanced photoacoustic H_2S gas sensor based on a fiber-amplifier source and a custom tuning fork with large prong spacing, Appl. Phys. Lett. 107 (2015), 111104.
[34] H. Zheng, Y. Liu, H. Lin, B. Liu, X. Gu, D. Li, B. Huang, Y. Wu, L. Dong, W. Zhu, J. Tang, H. Guan, H. Lu, Y. Zhong, J. Fang, Y. Luo, J. Zhang, J. Yu, Z. Chen, F. K. Tittel, Quartz-enhanced photoacoustic spectroscopy employing pilot line manufactured custom tuning forks, Photoacoustics 17 (2020), 100158.
[35] N. Maurin, R. Rousseau, W. Trzpil, G. Aoust, M. Hayot, J. Mercier, M. Bahriz, F. Gouzi, A. Vicet, First clinical evaluation of a quartz enhanced photo-acoustic CO sensor for human breath analysis, Sens. Actuators B Chem. 319 (2020), 128247.
[36] V. Spagnolo, R. Lewicki, L. Dong, F.K. Tittel, Quantum-cascade-laser-based optoacoustic detection for breath sensor applications, in: Proceedings of the 2011 IEEE International Symposium on Medical Measurements and Applications, 2011. ⟨DOI: 10.1109/MeMeA18236.2011⟩.
[37] H. Zheng, L. Dong, X. Yin, X. Liu, H. Wu, L. Zhang, W. Ma, W. Yin, S. Jia, Ppb level QEPAS NO_2 sensor by use of electrical modulation cancellation method with a high power blue LED, Sens. Actuators B Chem. 208 (2015) 173–179.
[38] Y. Ma, Y. He, Y. Tong, X. Yu, F.K. Tittel, Ppb-level detection of ammonia based on QEPAS using a power amplified laser and a low resonance frequency quartz tuning fork, Opt. Express 25 (23) (2017) 29356–29364.
[39] H. Wu, L. Dong, H. Zheng, X. Liu, X. Yin, W. Ma, L. Zhang, W. Yin, S. Jia, F.K. Tittel, Enhanced near-infrared QEPAS sensor for sub-ppm level H_2S detection by means of a fiber amplified 1582 nm DFB laser, Sens. Actuators B Chem. 221 (2015) 666–672.
[40] K. Sung, L.R. Brown, X. Huang, D.W. Schwenke, T.J. Lee, S.L. Coy, K.K. Lehmann, Extended line positions, intensities, empirical lower state energies and quantum assignments of NH_3 from 6300 to 7000 cm^{-1}, J. Quant. Spectrosc. Radiat. Transf. 113 (2012) 1066–1083.
[41] I. Mogilnicka, P. Bogucki, M. Ufnal, Microbiota and malodor—etiology and management, Int. J. Mol. Sci. 21 (2020) 2886.
[42] Y. Ma, Y. Hong, S. Qiao, Z. Lang, X. Liu, H-shaped acoustic micro-resonator-based quartz enhanced photoacoustic spectroscopy, Opt. Lett. 47 (3) (2022) 601–604.
[43] Y. Ma, Y. Hu, S. Qiao, Z. Lang, X. Liu, Y. He, V. Spagnolo, Quartz tuning forks resonance frequency matching for laser spectroscopy sensing, Photoacoustics 25 (2022), 100329.
[44] Y. He, Y. Ma, Y. Tong, X. Yu, Z. Peng, J. Gao, F.K. Tittel, Long distance, distributed gas sensing based on micro-nano fiber evanescent wave quartz-enhanced photoacoustic spectroscopy, Appl. Phys. Lett. 111 (2017), 241102.
[45] Y. Cao, Q. Liu, R. Wang, K. Liu, W. Chen, X. Gao, Development of a 443 nm diode laser-based differential photoacoustic spectrometer for simultaneous measurements of aerosol absorption and NO2, Photoacoustics 21 (2021), 100229.
[46] Y. Cao, R. Wang, J. Peng, K. Liu, W. Chen, G. Wang, X. Gao, Humidity enhanced N2O photoacoustic sensor with a 4.53 μm quantum cascade laser and Kalman filter, Photoacoustics 24 (2021), 100303.
[47] T. Wei, A. Zifarelli, S.D. Russo, H. Wu, G. Menduni, P. Patimisco, A. Sampaolo, V. Spagnolo, L. Dong, High and flat spectral responsivity of quartz tuning fork used as infrared photodetector in tunable diode laser spectroscopy, Appl. Phys. Rev. 8 (4) (2021), 041409.
[48] S. Li, J. Lu, Z. Shang, X. Zeng, Y. Yuan, H. Wu, Y. Pan, A. Sampaolo, P. Patimisco, V. Spagnolo, L. Dong, Compact quartz-enhanced photoacoustic sensor for ppb-level ambient NO_2 detection by use of a high-power laser diode and a grooved tuning fork. Photoacoustics 25 (2022) 100325.
[49] R. Lewicki, G. Wysocki, A.A. Kosterev, F.K. Tittel, Carbon dioxide and ammonia detection using 2 μm diode laser based quartz-enhanced photoacoustic spectroscopy, Appl. Phys. B 87 (2007) 157–162.

Zhijin Shang is now pursuing a Ph.D. degree in atomic and molecular physics in the Institute of Laser Spectroscopy of Shanxi university, China. His research interests include optical sensors and photoacoustic spectroscopy.

Shangzhi Li is now pursuing a Ph.D. degree in atomic and molecular physics in the Institute of Laser Spectroscopy of Shanxi university, China. His research interests include gas sensor, photoacoustic spectroscopy and laser spectroscopy techniques.

Biao Li is now pursuing a Ph.D. degree in atomic and molecular physics in the Institute of Laser Spectroscopy of Shanxi University, China. His research interests include gas sensors, photoacoustic spectroscopy, and laser spectroscopy techniques.

Hongpeng Wu received his Ph.D. degree in atomic and molecular physics from Shanxi University, China, in 2017. From 2015 to 2016, he studied as a joint Ph.D. student in the electrical and computer engineering department and rice quantum institute, Rice University, Houston, USA. Currently he is a professor in the Institute of Laser Spectroscopy of Shanxi University. His research interests include optical sensors and laser spectroscopy techniques.

Angelo Sampaolo obtained his Master degree in Physics in 2013 and the PhD Degree in Physics in 2017 from University of Bari. He was an associate researcher in the Laser Science Group at Rice University from 2014 to 2016 and associate researcher at Shanxi University since 2018. Since May 2017, he was a Post-Doctoral Research associate at University of Bari and starting from December 2019, he is Assistant Professor at Polytechnic of Bari. His research activity has included the study of the thermal properties of heterostructured devices via Raman spectroscopy. Most recently, his research interest has focused on the development of innovative techniques in trace gas sensing, based on Quartz-Enhanced Photoacoustic Spectroscopy and covering the full spectral range from near-IR to THz. His achieved results have been acknowledged by a cover paper in Applied Physics Letter of the July 2013 issue.

Pietro Patimisco obtained the Master degree in Physics (cum laude) in 2009 and the PhD Degree in Physics in 2013 from the University of Bari. Since 2018, he is Assistant professor at the Technical University of Bari. He was a visiting scientist in the Laser Science Group at Rice University in 2013 and 2014. Dr. Patimisco's scientific activity addressed both micro-probe optical characterization of semiconductor optoelectronic devices and optoacoustic gas sensors. Recently, his research activities included the study and applications of trace-gas sensors, such as quartz-enhanced photoacoustic spectroscopy and cavity enhanced absorption spectroscopy in the mid infrared and terahertz spectral region, leading to several publications, including a cover paper in Applied Physics Letter of the July 2013 issue.

Vincenzo Spagnolo obtained the PhD in physics in 1994 from University of Bari. From 1997–1999, he was researcher of the National Institute of the Physics of Matter. Since 2004, he works at the Technical University of Bari, formerly as assistant and associate professor and, starting from 2018, as full Professor of Physics. Since 2019, he is vice-rector of the Technical University of Bari, deputy to technology transfer. He is the director of the joint-research lab PolySense between Technical University of Bari and THORLABS GmbH, fellow member of SPIE and senior member of OSA. His research interests include optoacoustic gas sensing and spectroscopic techniques for real-time monitoring. His research activity is documented by more than 220 publications and two filed patents. He has given more than 50 invited presentations at international conferences and workshops.

Lei Dong received his Ph.D. degree in optics from Shanxi University, China, in 2007. From June, 2008 to December, 2011, he worked as a post-doctoral fellow in the Electrical and Computer Engineering Department and Rice Quantum Institute, Rice University, Houston, USA. Currently he is a professor in the Institute of Laser Spectroscopy of Shanxi University. His research activities research activities are focused on research and development in laser spectroscopy, in particular photoacoustic spectroscopy applied to sensitive, selective and real-time trace gas detection, and laser applications in environmental monitoring, chemical analysis, industrial process control, and medical diagnostics. He has published more than 100 peer reviewed papers with $>$ 2200 positive citations.